Technical Journal, University of Engineering and Technology (UET) Taxila, Pakistan Vol. 29 No. 4-2024
ISSN:1813-1786 (Print) 2313-7770 (Online)

Fabrication of Recycled Polyethylene Terephthalate Nanofibers (r-PET NFS) from Waste Bottles for Electrical Insulation Material.

N. Hussain[1], S. A. Noonari[2], U. Sarwar[3], S. Kaka[4], T. Hussain[5], G. B. Narejo[6]

[1]*Nano Fusion Technology Research Group, Division of Frontier Fibers, Institute for Fiber Engineering (IFES), Interdisciplinary Cluster for Cutting Edge Research (ICCER), Shinshu University, Tokida 3-15-1, Ueda, Nagano prefecture, 386-8567, Japan*
[2]*Isra University, Hyderabad Sindh, Pakistan*
[3,4]*Dawood University of Engineering and Technology, Karachi Pakistan*
[5]*Mehran University of Engineering and Technology, Jamshoro, Sindh, Pakistan*
[6]*NED University of Engineering & Technology, Karachi, Pakistan*

[1]engr.nadir712@hotmail.com

Abstract- In this study, recycled polyethylene terephthalate nanofibers (r-PET NFs) are produced from waste drinking plastic bottles via electrospinning technique to fabricate cost-effective and environment-friendly insulating material for electrical transformer. Nanofibers have the advantage of high surface area with low volume that enhances the insulating property of the material. Nanofibers have an advantage of high surface area that enhance the insulating property of the material. The insulating property of the r-PET NFs alone and oil-impregnated r-PET NFs were investigated using di-electric strength. Additionally, impedance spectroscopy was employed to optimize the insulation property of neat r-PET NFs and oil-impregnated r-PET NFs. The prepared r-PET NFs showed a maximum dielectric strength of 65 kV/mm for samples with thicknesses of 150 µm and 160 µm. When r-PET NFs impregnated with oil, resultant dielectric strength of 70 kV/mm at maximum thickness is achieved. The prepared r-PET NFs were more characterized by Fourier-transform infrared spectroscopy (FTIR), water contact angle (WCA), X-ray diffraction (XRD), thermogravimetric analysis (TGA) Scanning Electron Microscope (SEM),) and tensile test. The r-PET NFs showed excellent morphological, chemical, and mechanical properties to use as insulating material.

Keywords- Dielectric Strength; Nanofibers; Recycled PET; Electrospinning.

I. INTRODUCTION

Transformers are among the most crucial components of power networks. The performance of the transformers is essential for the power system to operate safely and steadily [1]. The life expectancy of a transformer is up to 25 years if it is operated in temperature range of around 65–95°C. In transformers, insulating oil is poured over dry paper to enhance its dielectric strength and cool the windings. [2].

In the 1940s, kraft paper was the only choice as a dielectric material for high voltage transformers. In the late 1950s, synthetic dielectric materials were introduced to replace the cellulose insulators. Currently, a blend of cellulose and synthetic materials is used for transformer insulation application [3]. Various insulating structures and composites have been developed. Aliphatic polyketone fibers exhibit excellent abrasion resistance, chemical resistance, heat resistance, low dielectric properties, and low water absorption [4]. The remarkable progress of nanotechnology in numerous industrial fields has greatly motivated researchers to develop advanced nanomaterials to enhance the performance and reliability of conventional materials. Currently, comprehensive research is focused on the application of nanotechnology for insulating materials in electrical transformers [5].

In this regard, nanofibers with outstanding performance can be a good candidate in this field. Power transformers with solid insulation were best served by cellulose insulation. In fact, it is not the best option, but its availability from natural renewable sources made it the preferred material [3]. So, if we find a material that is available and has plenty of sources, we can replace the cellulose with that material. Keeping, the excellent process ability and availability of polyethylene terephthalate (PET) has widened the scope of its use as insulators in shape of nanofibers, sheets, and films in various industrial applications. Nowadays PET is also used in health care applications like artificial blood vessels and heart valves [4]. All plastic products like plastic bottles, toys, and packaging materials are manufactured from PET.

The total consumption of products made from PET reach around 13 million tons [6]. PET products are economical and easily available, but PET products lead to environmental pollution. Many researchers are trying to change PET waste into products [7]. Zander et al fabricate PET nanofibers and used it as a water filter [8].

This research attempts to fabricate the more economical insulation material and reduce the time and energy through electrospinning of r-PET NFs. PET bottles were collected from waste drinking water bottles. Using r-PET NFS for electrical insulation applications will diminish waste disposal issues and subsequently provide a clean environment. This research analyzes the dielectric strength of r-PET NFS web to maintain neat and clean environment nanofibers for insulating material use. The polymer of polyethylene terephthalate for r-PET NFS was recycled from PET based drinking bottles and nanofibers were fabricated via the electrospinning technique. The physical, mechanical, and chemical properties of r-PET NFS webs were characterized using SEM, tensile machine, TGA, FTIR, and XRD.

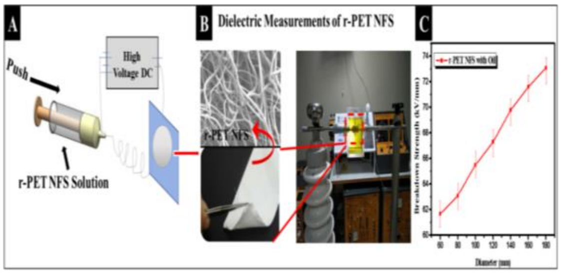

Figure 1. (A) Fabrication steps of r-PET NFS (B) Dielectric Measurements (C) Dielectric results.

II. Experimental

2.1 Materials

Recycled PET bottles without further purification are directly used to get r-PET NFs. Trifluoracetic Acid and Chloroform were acquired from Sigma Aldrich USA. Transformer oil was collected from Thermal power plant Jamshoro, Pakistan. Without additional purification, all materials were used.

2.2 Method

2.2.1 Fabrication of r-PET NFs

The process of electrospinning was used for the synthesis of the r-PET NFs. For this purpose, little pieces of PET (about 1 x 1 cm2) were cut, and then the pieces were dissolved in a 1:1 ratio of TFA to Chloroform to create a 15% w/w solution. The electrospinning was done using a high-voltage power source (Har - 100 * 12, Matsusada Co.; Japan). with a voltage supply of 15-20 kV and an interior diameter of 0.6 mm. The prepared solution was put into a syringe that had a capillary tip attached to it. Peeling off the r-PET NFS after electrospinning, they were let to dry overnight. Various thicknesses were achieved according to requirement.

2.2.2 SEM

The physical morphology of the pristine r-PET NFs, r-PET NFs after dielectric, and r-PET NFs submerged in oil were
seen using scanning electron microscopy (SEM) operating at a high voltage of 30 kV.

2.2.3 FTIR

The determination of chemical structural changes in neat r-PET NFS, r-PET NFS after dielectric, and oil immersed r-PET NFs, respectively. The samples were examined by Shimadzu, Japan, utilizing FTIR on IR prestige - 21.

2.2.4 XRD

The crystallinity of the neat r-PET NFs, r-PET NFs after dielectric and oil-immersed r-PET NFs were analyzed the high energy x-ray diffraction respectively at wide-angle x-ray diffractometer (WAXD). The apparatus was run with nickel-filtered CuKa radiation at 40 kV and 300 mA. At a scanning speed of 4°/min, the diffraction patterns were evaluated in the 10° to 60° degree range.

2.2.5 Di-electric Strength

The dielectric breakdown measurements were conducted according to the ASTM 149 standard and using Kyonan Elec. Co., Ltd, Japan device as shown in Figure 02. The test was performed under alternating current with boot speed of 0.1 kV per tap and frequency was set at 50 Hz. The voltage increased from zero onwards until the breakdown strength of the sample was achieved. The measurements were performed without oil and using mineral oil as a surrounding medium. To analyze the effect of thickness on breakdown strength variation, five different thicknesses of r-PET NFs were used to analyze breakdown strength. For every sample break down strength was calculated by equation (1).

$$E=V/t \tag{1}$$

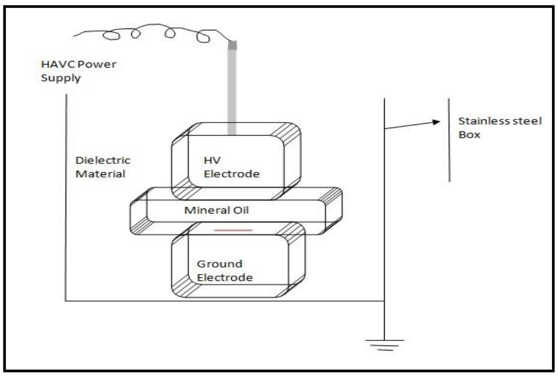

Figure 2. Diagram of Dielectric Electrodes

Where E is dielectric strength and t is the thickness of the sample and V is the breakdown voltage.

2.2.6 Impedance Spectroscopy

Dielectric properties of r-PET NFs with different thickness were measured by dielectric instrument analyser at room temperature. Dielectric instrument was attached with 1296 dielectric interface (solatron Analytical) and data extracted by computer and analyzed by Zview software. The variation in frequency was set from 10-1 to 106 Hz.

2.2.7 TGA

The rate of thermal degradation of neat r-PET NFs, r-PET NFs after dielectric and oil immersed r-PET NFs were performed with thermogravimetric analysis using thermo plus (TGA). The analysis was carried out in an air atmosphere with a heating rate of 10 °C/min and a temperature range of 0℃ to 500℃

2.2.8 Tensile Strength

The mechanical properties of the neat r-PET NFs, r-PET NFs after dielectric and oil immersed r-PET NFs were examined by Titan Universal Tester 3-910 Company Ltd, Germany. The ASTM D-638 standard was followed in measuring the tensile strength. The test was conducted at a speed of 5.0 mm/min. The values of young’s modulus and stress-strain curves was calculated by equations (2), (3) and (4) accordingly [9-10].

$$\varepsilon=\Delta l/l \quad (2)$$

$$\sigma = F/A \quad (3)$$

$$E = \sigma/\varepsilon \quad (4)$$

2.2.9. Shrinkage Test

The shrinkage test was analyzed by taking r-PET NFs sample’s size 5 cm2 with constant mean thickness 160µm at 90 ºC and the length of the r-PET NFs was compared before and after temperature, respectively. The shrinkage of r-PET NFs in both sides after temperature was calculated by using equations (5).

$$\text{Shrinkage (\%)} = (L\_1-L\_2)/L\_1 \times 100 \quad (5)$$

Where, L1 is the length of the fabric in each side before heat treatment and L2 is the length of the sample after heating.

III. Results and Discussion

3.1 Scanning Electron Microscopy

To determine the surface morphology before and after the di-electric process of neat r-PET NFs, r-PET NFs subjected to a dielectric process, and oil-immersed r-PET NFs have been analyzed by Scanning Electron Microscopy (SEM). The diameter of each sample was investigated via ImageJ software. The SEM images (Figures 2A and 2B) show that the neat r-PET NFs exhibit a bead-free, smooth morphology with an average nanofiber diameter of 800 nm. The nanofibers appear well-formed with no visible defects. r-PET NFs After the Dielectric Process, the r-PET NFs retained their flat and smooth morphology, as illustrated in Figures 2C and 2D no noticeable changes in the surface structure or diameter were observed, with the average diameter remaining at 800 nm. This suggests that the dielectric process did not affect the physical integrity of the nanofibers. Oil-Immersed r-PET NFs displayed a significant increase in nanofiber diameter, reaching an average of 1000 nm (Figures 2E and 2F). The SEM images reveal that the nanofibers absorbed substantial amounts of oil, which contributed to the increased diameter. Despite the absorption, the nanofibers maintained their overall smooth morphology without signs of structural degradation. SEM results highlight the structural stability of r-PET NFs under dielectric processing and their high absorption capacity in an oil-rich environment.

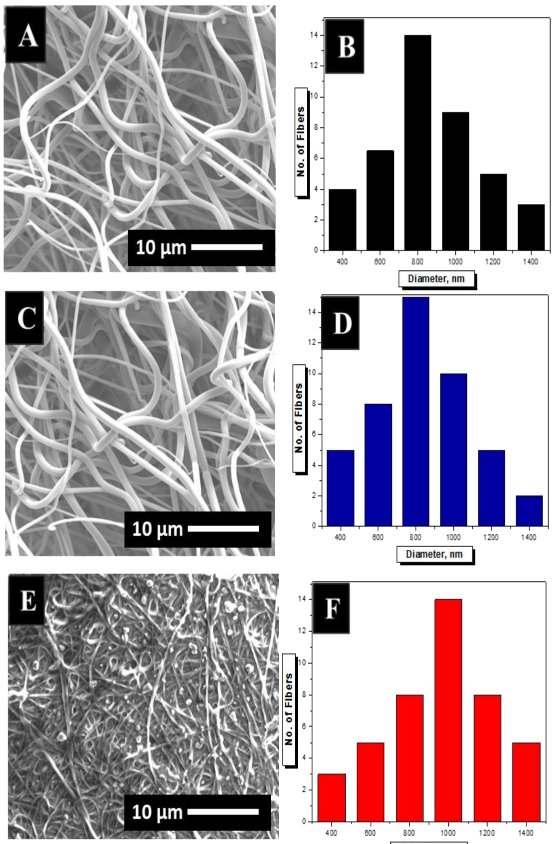

Figure 3. SEM images of (A) neat r-PET NFs (B) histogram of neat r-PET NFs A (C) SEM image of r-PET NFs after dielectric, (D) histogram of r-PET NFs after dielectric, (E) SEM image of oil immersed r-PET NFs (F) histogram of oil immersed r-PET NFs

3.2. FTIR Analysis of r-PET Nanofibers

The FTIR of the r-PET nanofibers (NFs) were analyzed under three conditions: (1) neat r-PET NFs, (2) r-PET NFs subjected to a dielectric process, and (3) oil-immersed r-PET NFs. The results of these evaluations are presented in Figure 4. The characteristic peaks of r-PET NFs were observed within the range of 2000–500 cm^{-1}, consistent with the expected diagnostic region for these r-PET NFs. These peaks confirmed the presence of the inherent functional groups in the r-PET structure. Following oil immersion, new peaks were identified at 2924 cm^{-1}, corresponding to the aliphatic C–H stretching vibrations of the oil. This observation indicates that the oil molecules interacted with the nanofiber surface. However, these interactions did not alter the fundamental chemical structure of the r-PET NFs, as no significant shifts or changes were detected in the primary characteristic peaks. This stability of the r-PET NFs' chemical structure despite the oil immersion demonstrates their robustness and compatibility for applications where exposure to oils or similar substances is expected.

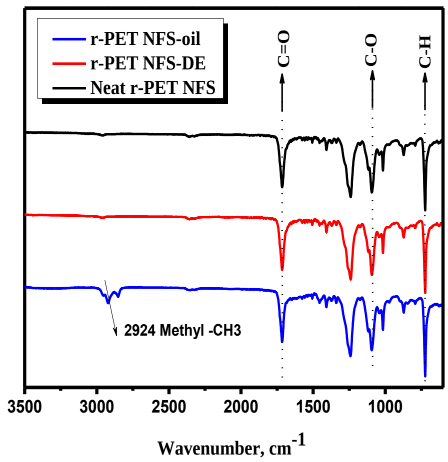

Figure 4. Chemical structure of neat r-PET NFs, r-PET NFs after dielectric, and oil immersed r-PET NFs

3.3. XRD Analysis of r-PET Nanofibers

The X-ray diffraction (XRD) patterns of neat r-PET NFs, r-PET NFs subjected to a dielectric process, and oil-immersed r-PET NFs—are shown in Figure 5. The XRD patterns of both neat and dielectric-processed r-PET NFs exhibit an intense peak at 20.1°, corresponding to a d-spacing of 4.6 Å. This peak is indicative of the crystalline structure inherent to r-PET. For the oil-immersed r-PET NFs, the primary peak at 20.1° remained unchanged, suggesting that the crystalline structure of r-PET was retained. However, a new peak was observed at 57.7°, which corresponds to a d-spacing of 5.2 Å. This additional peak is attributed to the presence of oil within the r-PET NFs, suggesting that oil molecules may have interacted with the material at the molecular level.

The XRD results also reveal a trend where a decreasing diffraction angle corresponds to an increase in the distance between molecules in the chemical bonds. This indicates that the oil's interaction with the r-PET NFs leads to slight structural modifications without disrupting the crystalline integrity of the material. These XRD results demonstrate the resilience of r-PET NFs in maintaining their structural properties even when exposed to oil, making them suitable for electrical insulation applications.

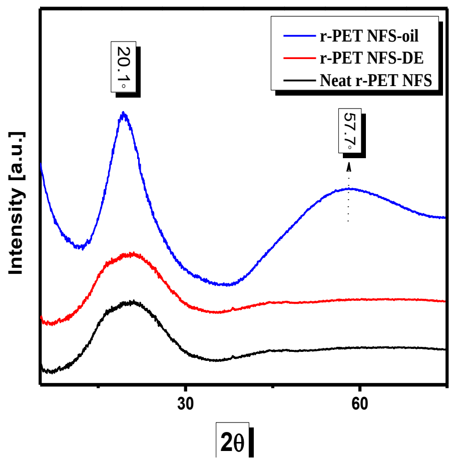

Figure 5. XRD patterns of neat r-PET NFS, r-PET NFS after dielectric and Oil Immersed r-PET NFS.

3.4. Dielectric Strength

Various samples of r-PET NFS were prepared with different thicknesses i.e. (50, 70, 140, 150, 160 µm,) to investigate the dielectric breakdown strength of the electrical insulation system. From Figure 6, thickness is the main parameter for insulation property. The increase in the thickness leads to higher dielectric breakdown strength and hence electrical insulation. The breakdown strength of different oil-immersed r-PET NFS with the same thicknesses was also measured at room temperature. The variation of the breakdown strength of oil-immersed r-PET NFS is shown in Figure 6B. It was shown that the breakdown strength of oil-immersed r-PET NFS was higher than that of non-immersed r-PET NFS. The comparison between Figures 6 A and B demonstrated that r-PET NFS gives more insulation and withstands high voltage when nanofibers are immersed in the oil. The recycled PET nanofibers (r-PET NFs) exhibited a maximum dielectric strength of 65 kV/mm for samples with thicknesses of 150 µm and 160 µm. However, beyond 160 µm, the dielectric strength plateaued and showed no further improvement. When impregnated with oil, the r-PET NFs achieved an impressive dielectric strength of 70 kV/mm at maximum thickness. This increase in dielectric strength highlights the excellent compatibility between r-PET NFs and oil. SEM analysis confirmed that the oil impregnation did not negatively impact the physical or mechanical properties of the r-PET NFs. Additionally, water contact angle measurements indicated that the hydrophobic nature of the r-PET NFs remained intact, with no damage caused by the oil. These findings demonstrate the robust performance of r-PET NFs, even in the presence of oil, making them highly suitable for advanced applications.

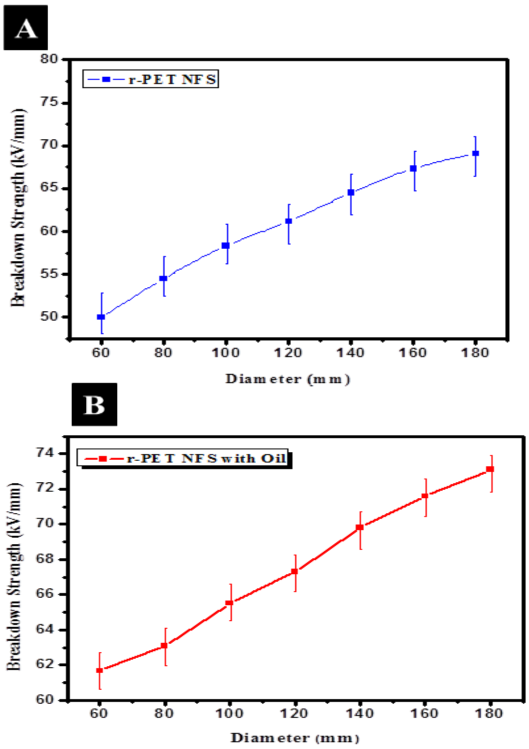

Figure 6. A Dielectric strength of r-PET NFS at different thickness. B Dielectric Strength of oil immersed r-PET NFS at different thickness

3.5 Impedance Spectroscopy

Relative permittivity was measured for nanofibers of different thicknesses at opposed frequencies at room temperature. Figure 7 (A) and (B) show the relative permittivity spectrum of the nanofibers. The frequency varies from 10-1 Hz to 106 Hz. In the given test ranges, it was observed that the high-thickness nanofibers have higher relative permittivity than those of small thicknesses. Furthermore, the relative permittivity of oil-impregnated nanofibers was also checked at the same frequency variations at room temperature. From Figure 7 B, the oil impregnation of the nanofibers did not affect the relative permittivity. Since the power transmitted and distributed globally is either 50Hz or 60Hz, this study also determines relative permittivity at a specific frequency.

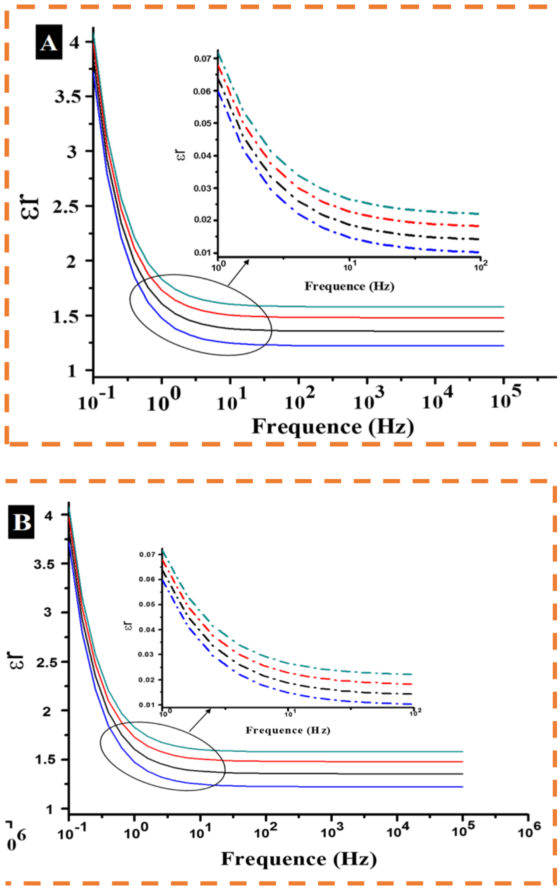

Figure 7. (A). Variation in relative permittivity of r-PET NFS with different thicknesses. (B). Variation in relative permittivity of oil-immersed r-PET NFS at different thickness

3.6. Water Contact Angel

The dynamic hydrophobic properties of neat r-PET NFS, r-PET NFS after dielectric and oil immersed r-PET NFS were analyzed by using dropping method with a contact angle as shown in Figure 8.

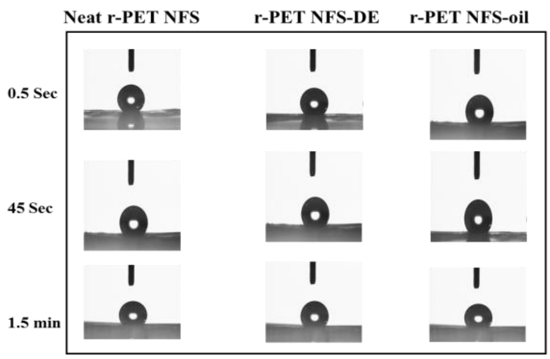

Figure 8. Results of dynamic contact angle of neat r-PET NFS, r-PET NFS after dielectric and oil immersed r-PET NFS

The water contact angle fulfils in time frame from 0.5 seconds to 1.5 minutes and it shows dynamic hydrophobicity between water and nanofiber membrane up to 130° at 1.5 minutes, it is due to superhydrophobic nature of r-PET NFS. As shows in figure 8 the dynamic hydrophobic contact angle property also examined for oil immersed r-PET NFS which revealed up to 120° at same time, respectively. In the view of above results r-PET NFS extremely recommended insulation material for transformer due to its superhydrophobic nature and mechanical strength

3.7. Thermal Gravimetric Analysis

The thermal gravimetric analysis of neat r-PET NFS, and oil immersed r-PET NFS were performed as shown in Figure 9. Probably due to adsorbed water and solvent molecules the initial weight loss is up to 350°C. The maximum weight loss occurred in the range of 370–4380C, which is related to the thermal degradation of nanofibers. Dry-type and liquid-filled transformers come in standard rises of 150 and 65 ℃, respectively [12]. As the decomposition temperature is much higher than the temperature of the transformer so, the prepared nanofibers with oil and without oil have great thermal stability and can be used as an insulator in transformer.

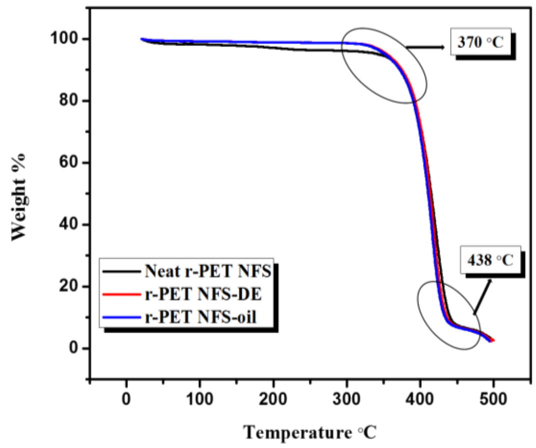

Figure 9. The thermal gravimetric analysis of neat r-PET NFS, and oil immersed r-PET NFS

3.8. Tensile Strength

Figure 10 A shows the mechanical strength of neat r-PET NFS, and oil-immersed r-PET NFS. The higher tensile strength belongs to the neat r-PET NFS. However, a small amount of the maximum load is lost while applying the oil. This may be because the oil causes greater slippage between the fibers, which lowers the load capacity by decreasing friction between the nanofibers. [13]. The mechanical characterization of r-PET NFS reveals that Young's modulus increases from 1.0 MPa to 1.2 MPa and remains unaffected on r-PETN NFS after being oil-immersed. This result shows excellent stability with heating in the transformer and oil as a surrounding medium to r-PET NFS. The results showed that the tensile strength did not significantly alter, indicating the high stability of the oil-impregnated nanofibers in the transformer as a surrounding medium.

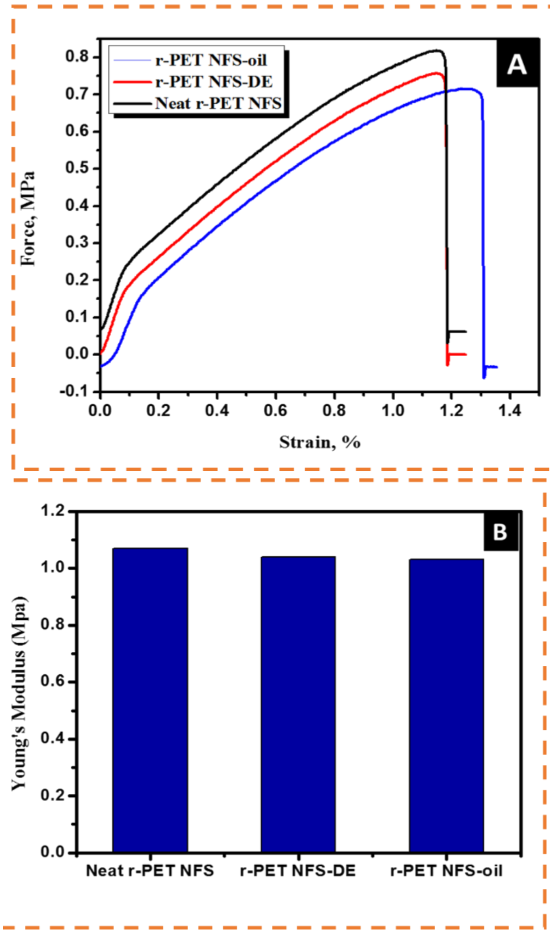

Figure 10. stress – strain curve and Young's Modulus of the neat r-PET NFS, and oil immersed r-PET NF

3.9. Shrinkage Test

Shrinkage values were determined using Equations 1 and 2. Table 1 presents the shrinkage parameters of r-PET nanofibers (NFs) subjected to dielectric testing and oil-immersed r-PET NFs. For the study, each sample was prepared with dimensions of 3×3cm².

Table. 1. Shrinkage study of r-PET nanofibers and r-PET nanofibers with oil

Shrinkage	r-PET NFS-DE	r-PET NFS-oil
Lengthwise	11%	13%
widthwise	9%	10.5%

[a] Shrinkage study was calculated by using eq. (1) and (1)

Significant shrinkage was observed in the samples when exposed to temperatures up to 120°C. The highest shrinkage was recorded in oil-immersed r-PET NFs, with a reduction of approximately 13% in length and 11% in width. In comparison, r-PET NFs tested after dielectric exposure exhibited

ISSN:1813-1786 (Print) 2313-7770 (Online)

relatively lower shrinkage, around 10%. These results suggest that both elevated temperatures and transformer oil can significantly impact the dimensional stability of r-PET NFs

3.10. Comparative Study

The comparative analysis highlights the exceptional performance of r-PET NFs as an insulation material. With a dielectric strength of 70 kV/mm (with oil) and 65 kV/mm (without oil), r-PET NFs outperform traditional materials such as Polyimide (7 kV/mm), PET Film (8 kV/mm), and even high-performance options like Ceramic (35 kV/mm). Despite their superior electrical insulating properties, r-PET NFs are the most economical, as they are derived from recycled drinking water bottles, significantly reducing material costs and promoting environmental sustainability. Furthermore, their comparable thermal conductivity (0.20 W/m·K) reinforces their versatility for electrical applications. This makes r-PET NFs a promising candidate for addressing both performance and waste disposal challenges in insulation technology. The proposed r-PET NFs exhibit superior dielectric strength and the lowest cost among the materials, demonstrating significant potential as an economical and high-performance insulation material

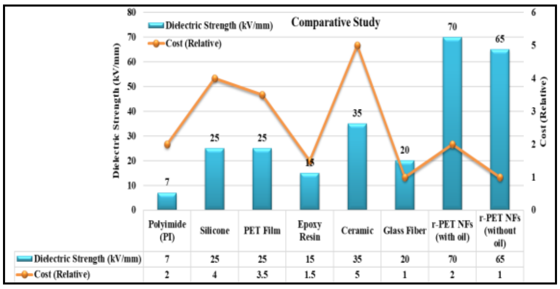

Figure 11. Comparative study of r-PET NFs and oil-immersed r-PET NFs with previously reported materials

IV. CONCLUSION

The r-PET NFS was successfully fabricated via electrospinning process and used as electrical insulation material for electrical transformer windings. The dielectric strength of r-PET NFS was investigated at different r-PET nanofiber thicknesses. It was also noticed that the immersion of r-PET NFS in oil increased the dielectric breakdown strength. The breakdown voltage of oil immersed nanofibers reached to 73.1 kV when the thickness reached to 180 µm. r-PET NFS showed good mechanical strength up to 0.8 Mpa. Furthermore, thermal degradation rate of r-PET NFS was 370℃ and r-PET NFS is a hydrophobic material; hence it will not absorb humidity which leads to improve the break down strength and lifetime of transformer. The results of present work show the development of a new generation of insulation for transformers thereby reducing the consumption of cellulose paper used in transformers. Furthermore, application of recycled PET to produce the nanofibers is environment-friendly and good for earth

REFERENCES

[1] Joseph T.M., Azat S., Ahmadi Z., Jazani O.M., Esmaeili A., Kianfar E., Haponiuk J., Thomas S. Polyethylene terephthalate (PET) recycling: A review. Case Stud. Chem. Environ. Eng. 2024;9:100673.

[2] Sin L.T., Tueen B.S. 1—Plastics and environmental sustainability issues. In: Sin L.T., Tueen B.S., editors. Plastics and Sustainability. Elsevier; Amsterdam, The Netherlands: 2023. pp. 1–43.

[3] Amobonye A.E., Aruwa C.E., Pillai S. Chapter 8—Biodegradability and current status of polyethylene terephthalate. In: Sarkar A., Sharma B., Shekhar S., editors. Biodegradability of Conventional Plastics. Elsevier; Amsterdam, The Netherlands: 2023. pp. 155–177

[4] Topuz, F.; Oldal, D.G.; Szekely, G. Valorization of Polyethylene Terephthalate (PET) Plastic Wastes as Nanofibrous Membranes for Oil Removal: Sustainable Solution for Plastic Waste and Oil Pollution. Ind. Eng. Chem. Res. 2022, 61, 9077–9086.

[5] Xiong, Q.; Tian, Q.; Yue, X.; Xu, J.; He, X.; Qiu, F.; Zhang, T. Superhydrophobic PET@ ZnO Nanofibrous Membrane Extract from Waste Plastic for Efficient Water-In-Oil Emulsion Separation. Ind. Eng. Chem. Res. 2022, 61, 11804–11814

[6] Hossain, M.T.; Shahid, M.A.; Ali, A. Development of nanofibrous membrane from recycled polyethene terephthalate bottle by electrospinning. OpenNano 2022, 8, 100089

[7] Djapovic, M.; Milivojevic, D.; Ilic-Tomic, T.; Lješevi´c, M.; Nikolaivits, E.; Topakas, E.; Maslak, V.; Nikodinovic-Runic, J. Synthesis and characterization of polyethylene terephthalate (PET) precursors and potential degradation products: Toxicity study and application in discovery of novel PETases. Chemosphere 2021, 275, 130005.

[8] Hashmi, M., Ullah, S., & Kim, I. S. (2019). Copper oxide (CuO) loaded polyacrylonitrile (PAN) nanofiber membranes for antimicrobial breath mask applications. Current Research in Biotechnology, 1, 1-10.

[9] Irfan, M. S., Gill, Y. Q., Malik, S., Naeem, M. T., Saeed, F., & Hashmi, M. (2019). Polyaniline-NBR Blends by in situ Polymerization: Application as Stretchable

Strain Sensors. Smart Materials and Structures.

[10] M. S. Irfan, Y. Q. Gill, M. Hashmi, S. Ullah, F. Saeed, and A. A. Qaiser, "Long-term stress relaxation behavior of Polyaniline-EPDM blends using the time-temperature-strain superposition method," Mater. Res. Express, vol. 6, no. 2, p. 025318, 2018.

[11] Contreras, J. E., Rodriguez, E. A., & Taha-Tijerina, J. (2017). Nanotechnology applications for electrical transformers—A review. Electric Power Systems Research, 143, 573-584.

[12] Mahar, F. K., Mehdi, M., Qureshi, U. A., Brohi, K. M., Zahid, B., & Ahmed, F., et al. Dyeability of recycled electrospun polyethylene terephthalate (pet) nanofibers: kinetics and thermodynamic study. Journal of Molecular Liquids. (2017)

[13] Mujahid Mehdia, Faraz Khan Mahara, Umair Ahmed Qureshia, Preparation of colorful r-PET nanofibers: physico-chemical studies. coloration Technology journal. 2017 CTE-17-0117

[14] Zander, N. E.; Gillan, M.; Sweetser, D. Recycled PET nanofibers for water filtration applications. Materials. 2016, 9(4), 247.

[15] Khatri, Z.; Ahmed, F.; Jhatial, A. K.; Abro, M. I.; Mayakrishnan, G.; Kim, I. S. Cold pad-batch dyeing of cellulose nanofibers with reactive dyes. Cellulose. 2014, 21(4), 3089-3095.

[16] Rantuch, P. E. T. E. R., & Chrebet, T. O. M. Á. Š. (2014). Thermal decomposition of cellulose insulation. Cellulose Chem. Technol, 48(5-6), 461-467.

[17] Khatri, Z.; Mayakrishnan, G.; Hirata, Y.; Wei, K.; Kim, I. S. Cationic-cellulose nanofibers: preparation and dyeability with anionic reactive dyes for apparel application. Carbohydrate polymers. 2013, 91(1), 434-443.

[18] Khatri, Z.; Khatri, A.; Saleem, U.; Mayakrishnan, G.; Kim, B. S.; Wei, K.; Kim, I. S Pad dyeing of cellulose acetate nanofibres with disperse dyes. Coloration Technology.2013, 129(2), 159-163.

[19] Khatri, Z.; Arain, R. A.; Jatoi, A. W.; Mayakrishnan, G.; Wei, K.; Kim, I. S. Dyeing and characterization of cellulose nanofibers to improve color yields by dual padding method. Cellulose. 2013, 20(3), 1469-1476.

[20] Dave, H.; Ledwani, L.; Chandwani, N.; Kikani, P.; Desai, B.; Nema, S. K.Surface Modification of Polyester Fabric by Non-Thermal Plasma Treatment and Its Effect on Coloration Using Natural Dye. Journal of Polymer Materials. 2013, 30(3), 291.

[21] Chen, Z.; Hay, J. N.; Jenkins, M. J. FTIR spectroscopic analysis of poly (ethylene terephthalate) on crystallization European Polymer Journal. 2012, 48(9), 1586-1610.

[22] Chandrashekar, R., Chaudhari, S. E., Bajpai, P. K., & Mehta, R. (2011). Developments in Insulating Paper for Power Transformers. J. Chem. Eng.

[23] Gilbert, R., Jalbert, J., Duchesne, S., Tétreault, P., Morin, B., & Denos, Y. (2010). Kinetics of the production of chain-end groups and methanol from the depolymerization of cellulose during the ageing of paper/oil systems. Part 2: Thermally-upgraded insulating papers. Cellulose, 17(2), 253-269.

[24] Sumin, L.; Kimura, D.; Yokoyama, A.; Lee, K.; Park, J. C.; Kim, I. The effects of laundering on the mechanical properties of mass-produced nanofiber web for use in wear. Textile Research Journal. 2009, 79(12), 1085-1090.

[25] Takami, K. M., & Mahmoudi, J. (2008). A novel study on the power transformer losses in relation to CO2 capturing technology. International journal of energy research, 32(12), 1151-1163.

[26] Prevost, T. A., & Oommen, T. V. (2006). Cellulose insulation in oil-filled power transformers: Part I-History and development. IEEE electrical insulation magazine, 22(1), 28-35.

[27] Wang, J.; Huang, N.; Yang, P.; Leng, Y. X.; Sun, H.; Liu, Z. Y.; Chu, P. K. The effects of amorphous carbon films deposited on polyethylene terephthalate on bacterial adhesion. Biomaterials. 2004, 25(16), 3163-3170.

[28] Mansour, S. H.; Ikladious, N. E. Depolymerization of poly (ethylene terephthalate) wastes using 1, 4-butanediol and triethylene glycol. Polymer Testing. 2002, 21(5), 497-505.

[29] Suh, D. J.; Park, O. O.; Yoon, K. H. The properties of unsaturated polyester based on the glycolyzed poly (ethylene terephthalate) with various glycol compositions. Polymer. 2000, 41(2), 461-466.

[30] Kamata, Y., Ohe, E., Endoh, K., Furukawa, S., Tsukioka, H., Maejima, M., & Hyohdoh, K. (1991). Development of low-permittivity pressboard and its evaluation for insulation of oil-immersed EHV power transformers. IEEE Transactions on electrical Insulation, 26(4), 819-825.

[31] Schroeder, S. M., & Michel, G. P. (1978). Washington, DC: U.S. Patent and Trademark Office. U.S. Patent No. 4,095,205.